

Peridynamic and continuum models of reinforced concrete lap splice compared

W. Gerstle, N. Sakhavand & S. Chapman

Department of Civil Engineering, University of New Mexico, Albuquerque, New Mexico, USA

ABSTRACT: Continuum mechanics originates with the linear elasticity model of Cauchy, developed in 1827. However, continuum mechanics fails when the displacement field becomes discontinuous and thus undifferentiable, as is the case with strain-softening, cementitious materials. To compensate for the inability of continuum mechanics to model cracking behavior, the discipline of fracture mechanics was developed in the twentieth century. The cohesive crack model is currently the most commonly used fracture model for cementitious materials. In 1998, the peridynamic (near-force) model was presented by Silling. In the peridynamic model, which is the logical extension of the cohesive crack model to the “cohesive particle model”, a nonlocal force interaction is assumed to take place between all pairs of infinitesimal particles within a neighborhood of finite size. The peridynamic pairwise force function completely defines the material behavior. The peridynamic model requires no derivative of the displacement field, and thus the displacement field need not be continuous. Therefore, cracks and other discontinuities can emerge unhindered as the solution progresses. Large deformations can be easily accommodated, as no kinematic strain assumptions need be made. This paper compares and contrasts the applicability of the peridynamic model and the continuum mechanics model to plain and reinforced concrete, and presents simulations and laboratory results of a lap-splice experiment.

1 INTRODUCTION

1.1 Background

The peridynamic model has been presented and discussed in previous papers (Silling 1998, Silling 2000, Silling 2002, Gerstle & Sau 2004, Gerstle et al. 2007a,b, Gerstle et al. 2005, Gerstle et al. 2007, Silling et al. 2007, Sau 2008). The basic premise of the peridynamic model is to describe material behavior as nonlocal force interactions between infinitesimal particles. Because the particles are of infinitesimal size, these force interactions are described on a per-volume basis. Thus, the peridynamic pairwise force function acting between two particles has units of force per-unit-volume-squared. Particle motion is simulated by integrating all forces acting on each particle to determine, via Newton’s second law, the acceleration of the particle. Knowing the particle’s acceleration, its velocity and position are updated using standard time-integration procedures.

The peridynamic model is not simply a molecular dynamics (MD) model for the following reasons. In MD, forces between atoms are functions only of relative atomic positions. On the other hand, with peridynamics, forces between particles depend upon an initial reference configuration. Also, in MD, inter-particle forces have no state, while in peridynamics, “links” between particles may have state, such

as plastic work or maximum prior tensile stretch. Also, peridynamics assumes a continuum material description of the reference configuration, while MD requires discrete atoms of finite mass.

Likewise, peridynamics is not a meso-mechanical model. In meso-mechanical models, materials are modeled at a lower-level scale, such as at the level of aggregate and cement mortar, for example as by Cusatis, Bazant and Cedolin (Cusatis et al. 2003, Cusatis & Bazant 2006). In such approaches, the concrete is modeled as a lattice or discrete set of interacting particles of finite size. The peridynamic model is not a particle or lattice model, because in the peridynamic model an infinite number of infinitesimal interacting particles are assumed. Although peridynamics may be discretized using particles, this discretization is not part of the peridynamic model, in the same sense that a finite element discretization is not a part of the continuum mechanics model. Indeed, discretization convergence studies can be conducted for both models. Convergence studies using meso-mechanical models, on the other hand, are difficult at best.

1.2 Scope of paper

This paper considers a difficult problem: computational simulation of a lap splice of two reinforcing bars embedded in concrete. This problem is difficult

because the behavior of the lap splice is strongly influenced by the fracture behavior of the surrounding concrete. Failure may occur by slip of the rebars with respect to the surrounding concrete accompanied by a zone of damaged concrete, which might in turn be surrounded by a combination of radial and longitudinal splitting cracks.

In Section 2, the lap splice problem investigated in this paper is defined. In Section 3, methods of solving the lap splice problem using continuum mechanics are discussed. In Section 4, the peridynamic solution to the problem is presented. Section 5 presents the laboratory results from the lap splice test. Section 6 presents the summary and conclusions.

2 LAP-SPLICE BENCHMARK PROBLEM

Figure 1 shows the lap-splice problem considered in this paper. The pair of 12 in. (30.48 cm) long, 1" (2.54 cm) diameter ribbed Dywidag bars are lapped by 6" (15.24 cm), and protrude 3" (7.62 cm) from each end of a standard 6" (15.24 cm) diameter by 12" (30.48 cm) long concrete cylinder. The bars are slightly eccentric to the specimen axis, as shown in Figure 1, and are separated by 0.5" (1.27 cm) clear distance. The Dywidag bars have a yield strength of 75 KSI (517 MPa), and the concrete has a uniaxial unconfined compressive strength of $f'_c = 4$ KSI (27.5 MPa), with 3/8" (0.95 cm) maximum aggregate size.

For simulation purposes, the following material properties are used for this benchmark problem:

Steel: Young's modulus $E = 29000$ KSI (200 GPa)
 Poisson's Ratio: $\nu = 0.3$
 Yield Stress: $F_y = 75$ KSI (517 MPa)
 Mass Density: $\rho = 15.22$ slug/ft³ (7850 kg/m³)
 Sound Speed: $c = 15130$ ft/s (4612 m/s)

Concrete: Young's modulus $E = 3504$ KSI (24.2 GPa)
 Poisson's Ratio: $\nu = 0.22$
 Tensile Strength: $f_t = 0.6$ KSI (4.13 MPa)
 Mass Density: $\rho = 4.50$ slug/ft³ (2400 kg/m³)
 Sound Speed: $c = 8310$ ft/s (2533 m/s)
 Fracture energy: $G_F = 1.0$ lb-in/in²
 (175.1 N-m/m²)

A downward velocity of 7.87 in/s (0.2 m/s) is applied to the bottom end of the reinforcing bar protruding from the bottom of the specimen and an equal upward velocity is applied to the top of the reinforcing bar protruding from the top of the specimen. The horizontal velocities of the 3" (7.62 cm) protruding ends of both reinforcing bars are prescribed to be zero.

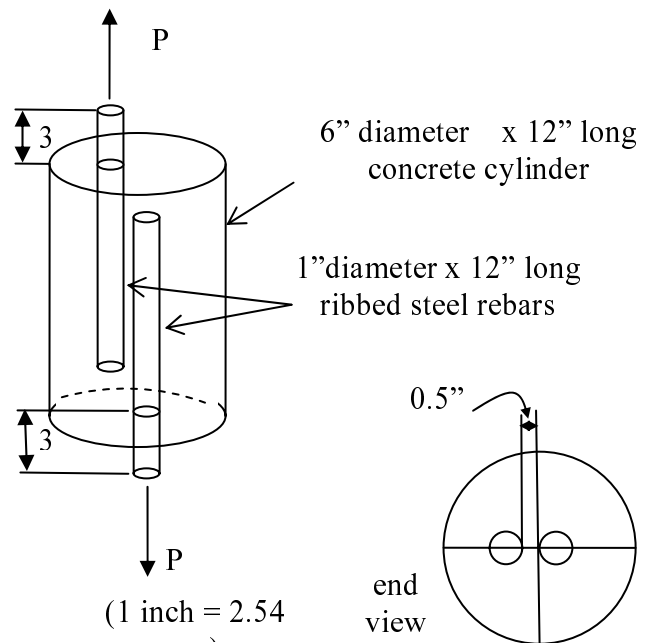


Figure 1. Lap splice benchmark problem geometry.

3 SOLUTION OF LAP-SPLICE PROBLEM WITH CONTINUUM MECHANICS

Because the lap-splice problem is fracture-sensitive, nonlinear continuum mechanics without augmentation with fracture mechanics has no hope of success. By augmenting continuum mechanics with a discrete fracture model, such as the cohesive crack model, the problem could perhaps be solved if a sufficient number of discrete cracks could be nucleated and propagated, as for example by Ingraffea and his co-workers (Carter et al. 2000). However, due to the large number of potentially interacting cracks at many size scales, the discrete crack approach seems unlikely to succeed. This paper poses the lap-splice problem as a challenge to discrete fracture mechanics modelers.

The problem can also be solved by continuum damage mechanics (Bazant 1991), using some form of a localization limiter in an attempt to correctly model the fracture energy. However, given the fact that damage is likely to be anisotropic and spatially inhomogeneous, most continuum damage mechanical theories, with their limiting assumptions, are insufficient to accurately model the problem. The problem of modeling interaction between the ribbed bar and the concrete, with a high degree of anisotropy and spatial inhomogeneity, is particularly difficult for continuum damage mechanics.

Complicating matters further is the fact that some of the cracking and damage is expected to progress dynamically, thus mandating a dynamic simulation capability.

Nonetheless, using a nonlinear implicit transient dynamics approach, but without a localization lim-

iter (except for the finite element size), an attempt was made to solve the lap splice problem using the commercial finite element code, ANSYS. The mesh employed is shown in Figure 2. Mirror symmetry boundary conditions are applied to the plane of symmetry to reduce the number of elements by a factor of two. ANSYS element solid65 was used to mesh the concrete and solid45 to mesh the steel bars; both are 8-noded brick elements, collapsed to tetrahedral elements. The stress-strain models for steel and concrete are similar to the material models described in Section 4, used in the Emu analysis.

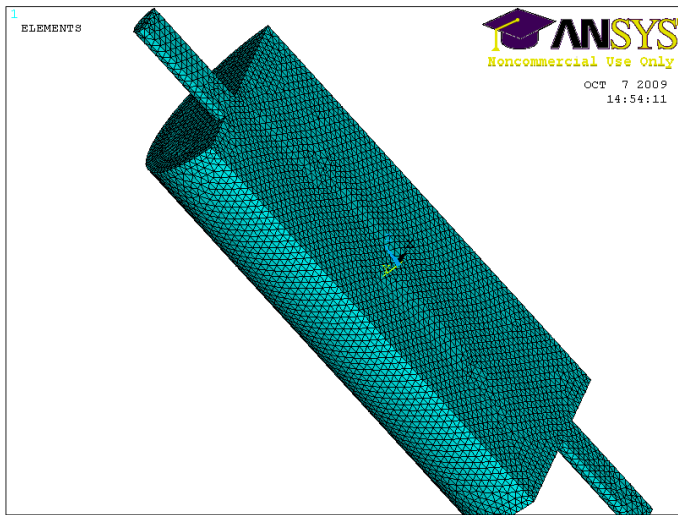


Figure 2. Finite element mesh.

Equal and opposite applied velocities of 0.2 m per second pulling the bars apart are applied. Figures 3, 4, and 5 show the von Mises strain distribution drawn on the deformed shape at three different times. Note that at 0.0022 s, as shown in Figure 5, in addition to large strains along the concrete-steel interface, a crack, evidenced by high strains, appears to be forming at the left-top of the concrete cylinder. Figure 6 shows a picture of concrete damage at 0.0026 s.

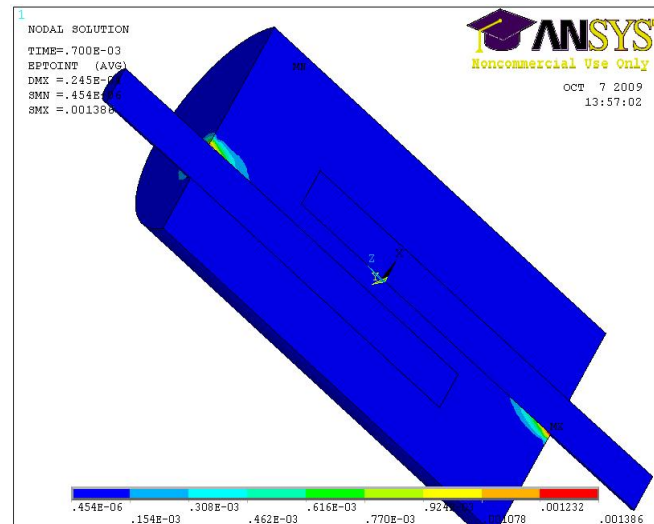


Figure 3. Von Mises strain distribution 0.0007 s.

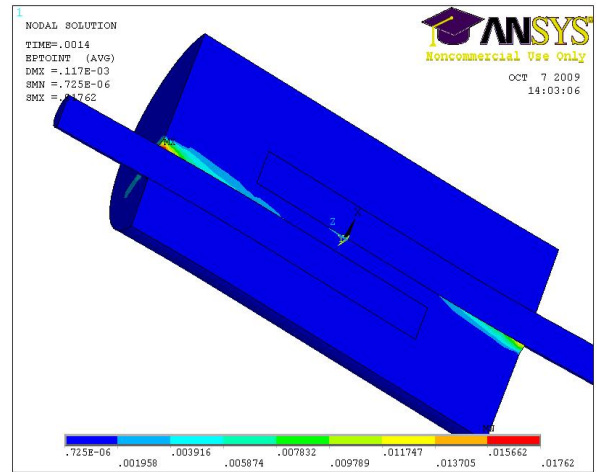


Figure 4. Von Mises strain distribution at 0.0014 s.

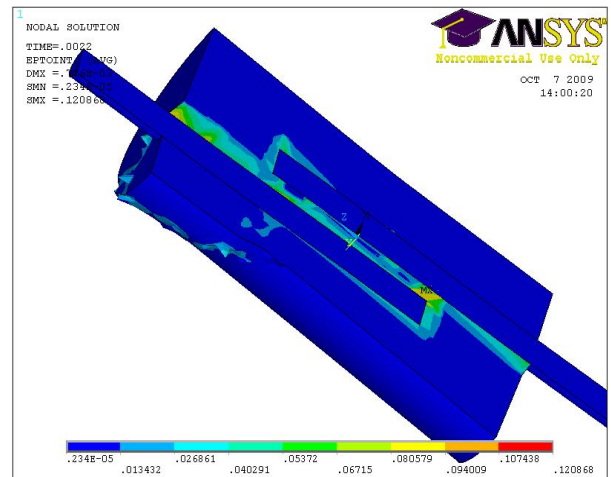


Figure 5. Von Mises strain distribution at 0.0022 s.

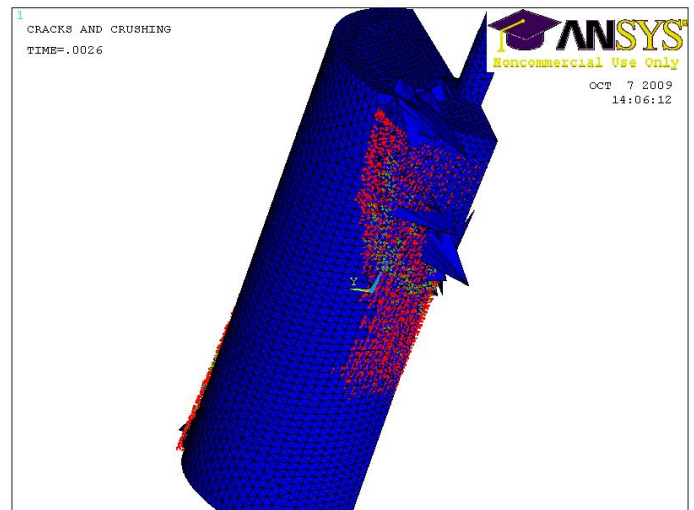


Figure 6. Concrete damage at 0.0026 s.

In this problem, there were 19186 nodes, 99121 elements, and 57558 degrees of freedom. The analysis was performed on a single processor, and required 15 hours of CPU time.

It is clear from Figure 6 that an area of localized damage has developed near the top of the specimen. Although this area is relatively smeared, it would probably have been more localized if the problem had been modeled using a finer mesh.

ANSYS does not support nonlocal continuum mechanics formulations, and therefore no attempt was made to perform a convergence study, as convergence cannot be achieved using a local continuum mechanics model.

4 SOLUTION OF LAP SPLICE PROBLEM WITH PERIDYNAMIC MODEL

4.1 Peridynamic model, EMU

EMU (Silling 1998) was used to simulate the lap splice problem using peridynamics. The quasi-cubical geometric region occupied by the steel and concrete is discretized with an array of equally-spaced discrete particles. Particles contained within the steel regions are given the characteristics of steel, while particles contained within the concrete regions are given the characteristics of concrete. Particles not within a material region are discarded.

The steel and concrete both possess the peridynamic pairwise force relations shown in Figure 7. With reference to Figure 7, the peridynamic constants (indicated with a ‘) are calculated from macro material parameters using the following formulas:

$$E' = \frac{6E}{\pi \delta^4 (1-2\nu)} \quad (\text{from Aguilera 2008});$$

$$G' = \frac{5G_F}{\pi \delta^5} \quad (\text{from energy considerations});$$

$$\varepsilon'_y = \frac{F_y}{2E} \quad (\text{micro yield is half of macro yield strain});$$

$$\varepsilon'_c = \frac{G'}{E' \varepsilon_y} + \frac{\varepsilon'_y}{2} \quad (\text{from consideration of energy}).$$

in which the material horizon, δ , is equal to 3.015 times the grid spacing, indicating that each interior particle interacts with 122 other particles.

To simulate the toughening effect of the ribs on the steel bars, the peridynamic force relation between concrete and steel particles is increased by setting the peridynamic bond force to three times the peridynamic force for concrete. Also the peridynamic bond strength of such bonds is set to three times the bond strength of concrete.

To prevent the two rebars from “sticking” together, the peridynamic forces between the two bars are assigned to be null.

Figure 8 shows the magnified deformed shapes at three simulation times. It is clear from the simulation that subsequent to crack nucleation and propagation, a number of fragments of concrete are splitting off of the specimen, ultimately allowing the top reinforcing bar to break off of the specimen. Note that the bottom portion of the top bar is also pulling out of the concrete specimen.

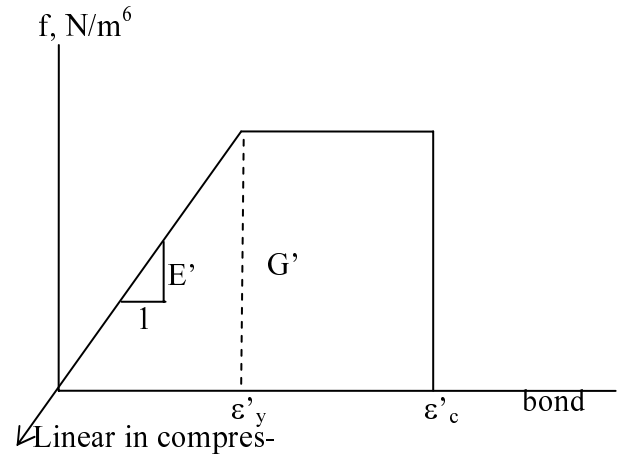


Figure 7. Peridynamic pairwise force functions.

This simulation was blind in that it was performed before the laboratory test, described in Section 5, was performed.

4.2 Emu computational performance

“Nano”, a linux cluster housed at the UNM Center for Advanced Research Computing, was used for our simulations. Nano is rated at 1300 GFLOPS, has one head node and 36 compute nodes, with two Intel Xeon 5140 2.33 GHz CPU’s per node with two cores per CPU, with Myrinet interconnect between the compute nodes.

To date, EMU was used to solve the lap splice problem with a maximum of 493,344 particles, with various discretizations as shown in Table I. Figure 8 shows damage and deformed shapes at three times in the simulation for the finest (493,344-particle) discretization.

Table 1. EMU Grid and particle discretization of lap splice problem.

Number of grid points			Grid spacing (m)	Number of particles
x	y	z		
33	33	69	0.00500	73,355
44	44	92	0.00375	185,314
65	65	137	0.00250	493,344

If the processor- communication overhead is small, the solution wall-time, T, is estimated as

$$T = K \times \frac{N \times C}{P} \quad \text{Eq. 1}$$

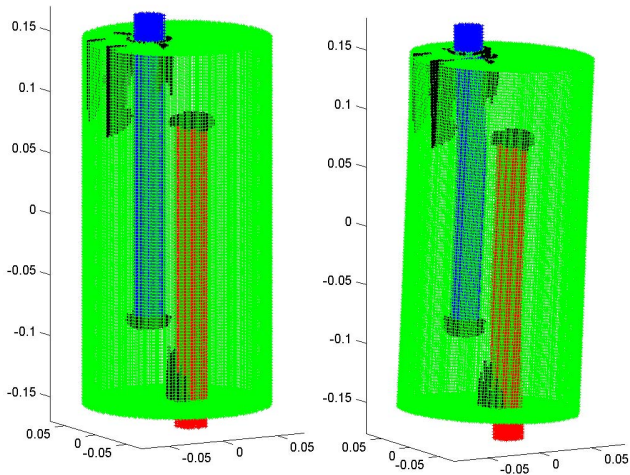
where K = 1.8x10⁻⁴ CPU-seconds per particle-time step

P = number of CPUs

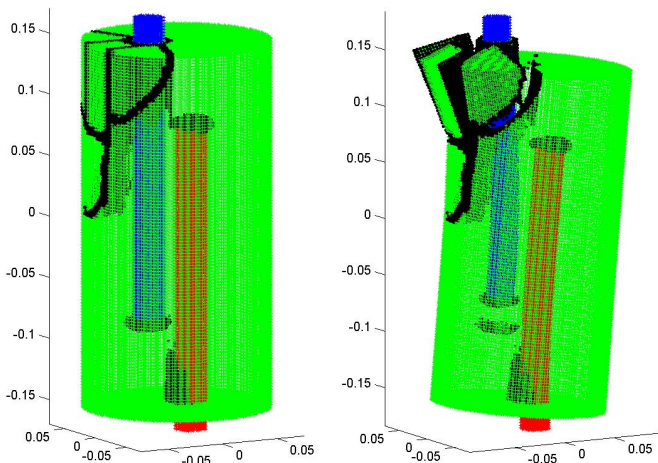
N = total number of particles

C = number of simulation time steps

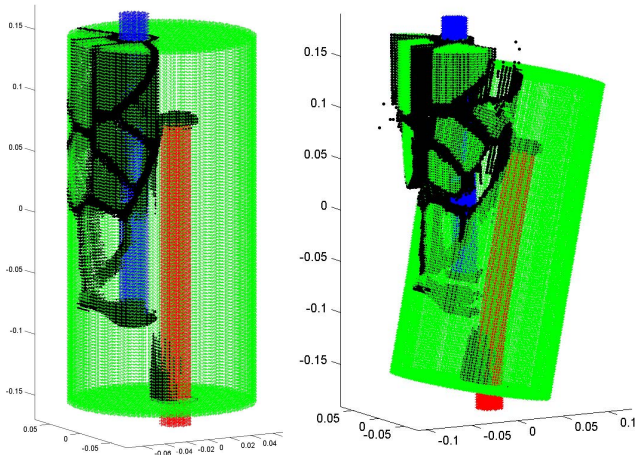
The number of time steps required to solve a peridynamic problem using EMU is dependent upon the time step size and upon the time required to arrive at a static solution.



t = 0.00072 s
(a)



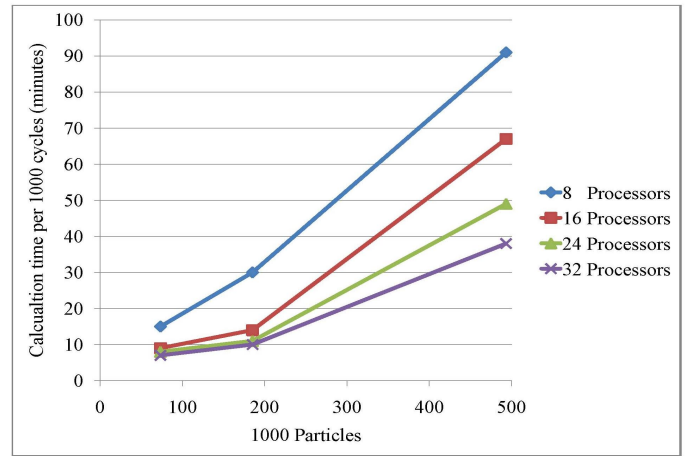
t = 0.0014 s
(b)



t = 0.0022 s
(c)

Figure 8. Undeformed (left) and deformed (right) shapes at three simulation times from peridynamic (EMU) simulation. Deformation is magnified by a scale factor of 50. Particles with more than 30% of peridynamic links being broken are displayed as black.

Table 2. Computational Performance of Emu for lap splice problem.



Assuming the simulation time, T_s , required to arrive at a solution is equal to the highest natural period of the initial system, and the time step size is approximately one-tenth of the lowest natural period of the system, one can predict how large a problem can be solved in a reasonable time (say, in 24 hours, using 32 processors).

For solution stability, the time step is selected by EMU to be one-third the particle spacing divided by the maximum sound velocity. Thus, as particle spacing, s , is decreased, time step, dt , decreases proportionately.

$$T = \frac{K}{P} \times \left(\frac{V}{s^3}\right) \times \left[\frac{T_s}{(s/3c)} \right]. \quad \text{Eq. 2}$$

For reinforced concrete problems, modeled with a peridynamic grid discretization, one can, for example, assume:

grid spacing, $s = 0.005$ m (approximately the aggregate size)

number of processors, $P = 32$

sound speed in steel, $c = 4612$ m/s

simulation duration, $T_s = 0.005$ s

solution time, $T = 24$ hours = 86,400 s

Solving for the volume, V , of the problem

$$V = \frac{TP}{K \left(\frac{3cT_s}{s^4}\right)} = \frac{(86,400)P}{(1.8 \times 10^{-4}) \left(\frac{3 \times 4612 \times 0.005}{0.005^4}\right)} = 0.00434P$$

The volume of the problem that can be modeled is roughly proportional to the number of available CPUs. If 8 processors are available, the maximum problem volume that can be modeled in 24 hours is 0.0347 m^3 , or a cube approximately 0.33 m on a side. If 1000 processors are available, the volume

that can be reasonably modeled in 24 hours is 4.34 m^3 , or a cube approximately 1.6 m on a side.

Aside from the time required for the computation, there is also the question of memory storage. With today's hard disk capacity easily surpassing more than 100 Gbytes of storage, it appears that disk storage is not a limiting factor; rather time of execution is the limiting factor.

Thus, by using today's massively parallel computers, it is possible to model 3D reinforced concrete components of significant size (such as parts of beams and columns, and connections) using the peridynamic model. However, modeling entire buildings or bridges using peridynamics is not currently feasible.

5 LABORATORY TESTING

Laboratory experiments were performed after the peridynamic simulations were concluded in order to evaluate the predictive value of the simulations. Three concrete cylinders with embedded, lapped, Dywidag bars, with geometry as shown in Figure 1, were cast from 4000 psi Quick-Crete Redimix, along with six 4" (10.16 cm) diameter by 8" (20.32 cm) long concrete cylinders for determination of uniaxial tensile compressive strength, f'_c . Three of the compression cylinders were tested at 7 days after casting, and f'_c was found to be 2837 PSI with a standard deviation of 190 PSI.

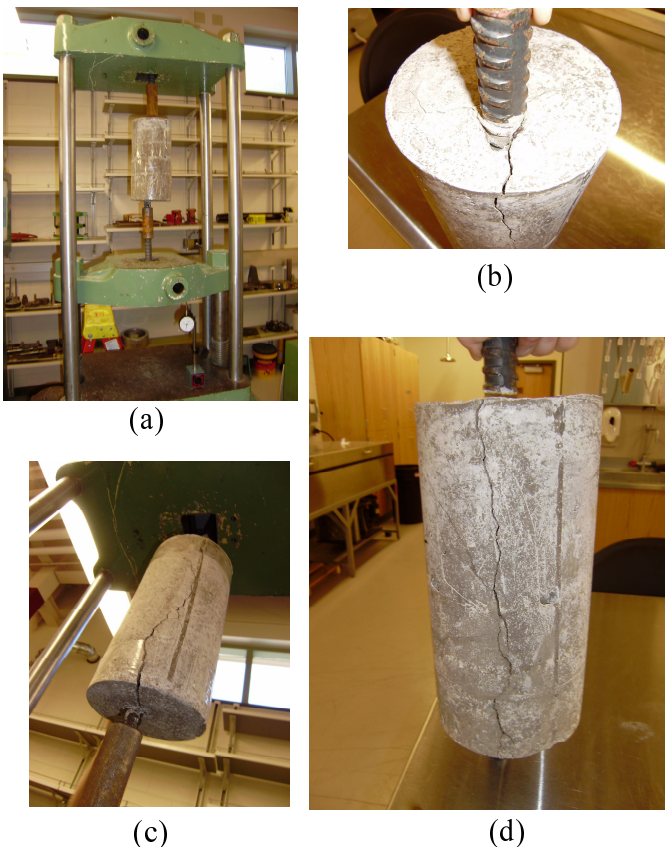


Figure 9. Photographs of lap-splice specimens.

The lap-splice specimens were also tested seven days after casting in tension under stroke control.

The crack patterns of all three specimens were approximately identical: two or three longitudinal splitting cracks with each crack approximately coplanar with the axis of the concrete cylinder, as shown in Figure 9. The cracks were observed to initiate at the tops of the specimens, as was predicted by the simulations. The load-displacement curves up to failure are shown in Figure 10.

The crack patterns from laboratory testing are somewhat different than the peridynamic simulation results. These results are currently not fully understood. The laboratory tests were loaded much more slowly, at $1 \times 10^{-6} \text{ m/s}$, than the simulations, in which the loading rate was quite dynamic, at 0.2 m/s. The difference in loading rate may be one reason for the differing failure modes. Running the simulation at the rate that the laboratory test was conducted is not feasible using EMU, due to the required small time steps. Also, shrinkage and creep effects were not included in the ANSYS and EMU simulations.

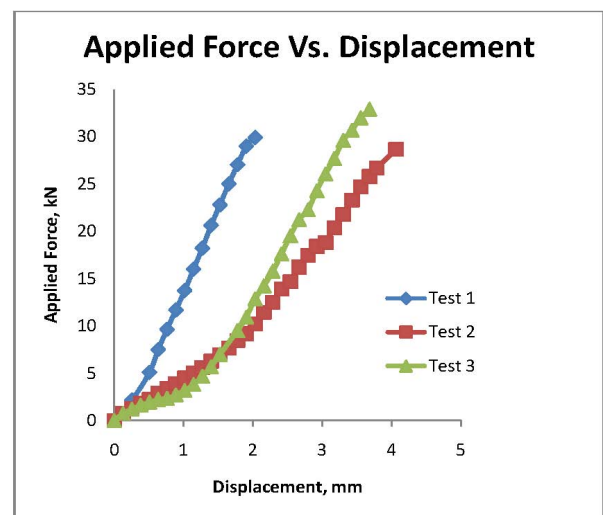


Figure 10. Force vs. Displacement from Laboratory Tests.

6 CONCLUSIONS

Although the research in 3D peridynamic modeling of reinforced concrete is in its infancy, there are many potential advantages in using the peridynamic approach to model quasibrittle cementitious materials like concrete.

The peridynamic model is the logical extension of the cohesive crack model, where, rather than cohesive surfaces, there are cohesive particles.

While it is true that continuum mechanics has been very successful for modeling elasticity and plasticity, continuum damage mechanics has not been as successful. The reason is that damage inherently localizes, and without a localization limiter, it is not possible to obtain a converged solution using

local continuum mechanics concepts. While many researchers have developed nonlocal continuum mechanics formulations, it is far more direct to avoid making an assumption of continuous displacements in the first place.

Overall, a reasonably successful simulation of a lap splice was created using EMU. While the solution is not perfectly in alignment with the laboratory results, some features later observed in the laboratory were well simulated. Specifically, in both the simulation and in the laboratory, cracks formed, resulting in a fragmented specimen, which allowed the rebar to pull out. Although the fragments observed in the simulation do not match the character of the fragments observed in the laboratory very well, by developing better peridynamic constitutive models (including shrinkage, rate and history effects), it will be possible to better simulate reinforced concrete problems in the future.

This paper has shown that by using EMU, problems of significant size can be simulated, but massively parallel computers are required at present for simulating 3D problems.

The lap splice problem posed is a challenging benchmark problem, and the authors would like to see other researchers apply their simulation techniques to it.

ACKNOWLEDGMENTS

Special thanks to Stewart Silling, of Sandia National Laboratories, for sharing the code, EMU, and for helping us to install the code on the University of New Mexico's high performance computers.

The UNM Center for Advanced Research Computing provided the computing facilities for this work.

REFERENCES

- Aguilera, E., 2008. MS Thesis, Department of Civil Engineering, University of New Mexico.
- Bazant, Z. P. 1991, "Why Continuum Damage is Nonlocal: Micromechanics Arguments", *Journal of Engineering Mechanics*, Vol. 117, No. 5, pp. 1070-1087.
- Carter, B.J., Wawrzynek, P.A., Ingraffea, A.R., 2000, "Automated 3D Crack Growth Simulation", *Gallagher Special Issue of Int. J. Num. Meth. Engrg.*, 47, pp. 229-253.
- Cusatis, G. and Bazant, Z. and Cedolin, L. 2003. "Confinement-shear lattice model for concrete damage in tension and compression I: theory", *J. of Engrg. Mech. ASCE* 129(12), 1439-48.
- Cusatis, G. and Bazant, Z., 2006. "Size Effect on compression fracture of concrete with or without V-notches: a numerical meso-mechanical study", *Computational Modelling of Concrete Structures*, Meschke et al. eds., Taylor and Francis Group, London.
- Gerstle, W. and Sau, N., 2004. "Peridynamic Modeling of Concrete Structures", *Proceedings of the Fifth International Conference on Fracture Mechanics of Concrete Structures*, Li, Leung, Willam, and Billington, Eds., Ia-FRAMCOS, Vol. 2, pp. 949-956.
- Gerstle, W. H., Sau, N., and Aguilera, E., 2007a. "Micropolar Modeling of Concrete Structures", *Proceedings of the Sixth International Conference on Fracture Mechanics of Concrete Structures*, Ia-FRAMCOS, Catania, Italy, June 17-22.
- Gerstle, W., Sau, N., and Aguilera, E., 2007b. "Micropolar Peridynamic Constitutive Model for Concrete", *19th Intl. Conf. on Structural Mechanics in Reactor Technology (SMiRT 19)*, Toronto, Canada, August 12-17, pp. B02/1-2.
- Gerstle, W., Sau, N., and Silling, S., 2005. "Peridynamic Modeling of Plain and Reinforced Concrete Structures", *18th Intl. Conf. on Structural Mechanics in Reactor Technology (SMiRT 18)*, Atomic Energy Press, Beijing China, August 7-12.
- Gerstle, W., and Sau, N., and Silling, S., 2007. "Peridynamic Modeling of Concrete Structures", *Journal of Nuclear Engineering and Design*, No. 237, pp. 1250-1258.
- Sau N., 2008. "Peridynamic modeling of quasibrittle structures", *Doctoral Dissertation*, University of New Mexico.
- Silling, S. 1998. "Reformulation of Elasticity Theory for Discontinuities and Long-Range Forces". SAND98-2176, Sandia National Laboratories, Albuquerque, NM.
- Silling, S. 2000. "Reformulation of Elasticity Theory for Discontinuities and Long-Range Forces". *Journal of the Mechanics and Physics of Solids* 48: 175-209.
- Silling, S. 2002. "Dynamic Fracture Modeling With a Mesh-free Peridynamic Code". SAND2002-2959C, Sandia National Laboratories, Albuquerque, NM.
- Silling, S.A., Epton, M., Weckner, O., Xu, J., and Askari, E., 2007. "Peridynamic States and Constitutive Modeling", *J. Elasticity*, 88, pp. 151-184.